atmosphere

MDPI

Article

High-Altitude Discharges and Whistlers of Volcanic Thunderstorms

Evgeniy I. Malkin [1,*,†], Boris M. Shevtsov [1,†], Nina V. Cherneva [1], Evgeniy A. Kazakov [1,*] and János Lichtenberger [2,3]

[1] Institute of Cosmophysical Research and Radio Wave Propagation FEB RAS, 684034 Paratunka, Russia; nina@ikir.ru (N.V.C.)
[2] Department of Geophysics and Space Sciences, Eötvös University, H-1117 Budapest, Hungary; lityi@sas.elte.hu
[3] Space Research Group, Hungarian Research Network (HUN-REN), Eötvös Loránd University (ELTE), H-1117 Budapest, Hungary
* Correspondence: malkin@ikir.ru (E.I.M.); kazakov@ikir.ru (E.A.K.)
† These authors contributed equally to this work.

Abstract: The results of the observations of atmospherics and whistlers initiated by high-altitude electrical discharges that occurred during the eruption of the Kamchatka volcanoes (Bezymianny and Shiveluch (Russia))on 7 and 10 April 2023 are presented. Recording of atmospherics and associated whistlers was carried out by a VLF (very low frequencies) radio direction finder. Two-hop whistlers were identified by dispersion coefficient, which corresponded to the double passage of the signal from Kamchatka to Australia and back. The heights of the electric discharges were determined by means of interferograms of direct and reflected from the ionosphere radiofrequency atmospherics. The high-altitude distribution of an electric discharge is obtained, the penetration of which into the ionosphere is responsible for the generation of whistlers. The characteristics of volcanic electrical discharges and whistlers can be used to estimate the height of an explosive eruption.

Keywords: high-altitude discharges; whistlers; volcanic thunderstorms; VLF direction finder

Citation: Malkin, E.I.; Shevtsov, B.M.; Cherneva, N.V.; Kazakov, E.A.; Lichtenberger, J. High-Altitude Discharges and Whistlers of Volcanic Thunderstorms. *Atmosphere* **2024**, *15*, 1503. https://doi.org/10.3390/atmos15121503

Academic Editors: Masashi Kamogawa and Yoav Yair

Received: 17 October 2024
Revised: 11 December 2024
Accepted: 14 December 2024
Published: 17 December 2024

1. Introduction

Eruptive clouds that occur during volcanic eruptions create thunderstorm and ash hazards. Due to the need to assess the scale of these threats, monitoring of the power and dynamics of eruptive clouds is important. The solution of these remote sensing problems is possible through integrated radio observations of the thunderstorm activity of eruptive clouds using WWLLN [1] and the VLF radio direction finder [2]. Unlike visual observations, radio observations do not have critical dependence on weather conditions and time of a day.

WWLLN is used to detect and track eruptive clouds [3–6]. The intensity of the thunderstorm activity can be used to judge the power of the eruption. AWDANet [7,8] allows us to identify whistlers that are generated above eruptive clouds, which propagate to the magnetically conjugated point and return. Whistler generation is associated with high-altitude lightning, the ratio of the altitude to the total number of volcanic lightning electrical discharges, which allows us to determine the dynamics of the formation of eruptive clouds and the height of the rise of eruptive material.

1.1. Electrification of Eruptive Clouds

Dynamics of eruptive cloud formation and, as a consequence, the mechanism of formation of electric charge on the cloud upper edge differ from the electrification process in meteorological clouds. It has been shown in the papers [3,9–11] that magma fragmentation (destruction) in the crater channel plays an important role in eruptive cloud electrification. Charge formation is also possible during the injection of an ash–gas jet into the atmosphere when they break during particle collisions [3]. It is assumed that multiple crater discharges,

which generate continuous electromagnetic noise, are associated with this charging mechanism (commonly referred to as the continual radio frequency or CRF) [12,13]. When an eruptive column reaches its maximum height, an eruptive cloud is formed under the wind stratification conditions. In this cloud, the electrification process causes the formation of electric charges just like in meteorological clouds. The similarity of these processes is explained by the content of erupted material, up to 7% of the mass content of which is water. Ash particles act as condensation nuclei, which form hailstones when they come in contact with supercooled water [14,15].

Based on the natural observations of the atmospheric electric field potential gradient of the Great Tolbachik Fissure Eruption in July–October 1975 (Kamchatka Peninsula, Kamchatka, Russia) [9] (Figure 1a), and of the vulcano Sakurajima (Japan) during its eruptions in 1991 [16] (Figure 1b) and 1995 [10] (Figure 1c), phenomenological schemes of volumetric charge separation during eruptive column formation and eruptive cloud propagation were proposed.

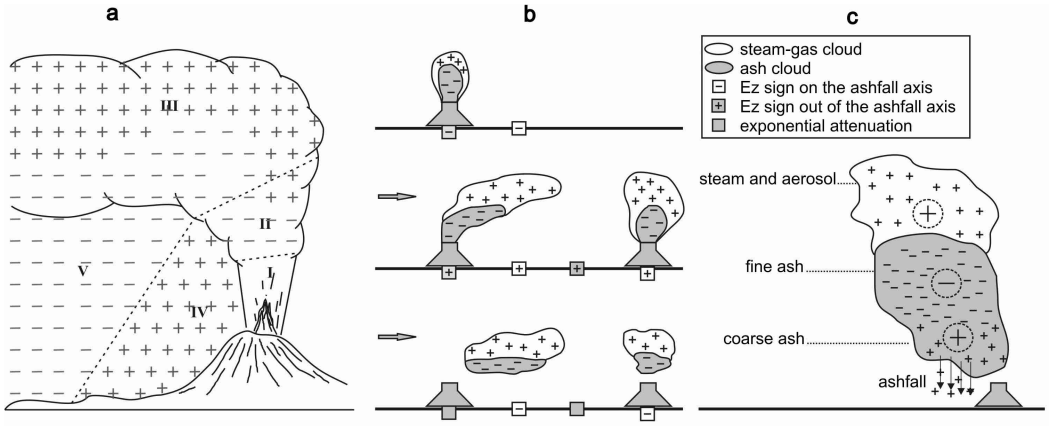

Figure 1. Proposed phenomenological schemes of volumetric charge separation during eruptive column formation and eruptive cloud propagation. (**a**) Adapted from Rulenko: I—charge separation under gravity force at the initial section in case of weak wind; II—formation of a cloud at the automodel section under wind effect; III—plume in the floating zone; IV—region of coarse fraction fall; V—region of tephra fall [9]. (**b**) Adapted from Lane [16]. (**c**) Adapted from Miura [10].

Charge distribution in an eruptive cloud was explained by eolian differentiation and dejecta sedimentation in the gravity field. Such a separation of charges under the impact of atmospheric wind stratification conditions and under the gravity field conditions agrees with the known phenomenological feature of bipolar particle charging depending on their size (SDBC). In this case, the negative charge is typical for small particles and the positive charge is typical for larger ones [12].

1.2. The Explosive Volcanic Eruption and Thunderstorm Activity

In the paper [17], the authors discuss volcano eruptions from the point of view of accompanying lightning activity. Two types of scenario were distinguished.

In the "soft" scenario, an eruptive cloud is formed at the tropopause height and is explained by positive buoyancy of the ash–gas mixture. The electric structure is completely described by the phenomenological scheme illustrated in Figure 1b). To form a high-altitude discharge, it is necessary to neutralize the positive charge of the aerosol located at the upper edge of the eruptive cloud. Therefore, in this case, a pair of positive discharges should be observed, cloud–earth and ionosphere–cloud. In this way, volcanic thunderstorms are similar to meteorological ones. Manifestations in the optical range of high-altitude discharges or lightning between the ionosphere and the cloud are called sprites, which in this work are observed using an VLF radio direction finder.

The "hard" scenario is explained by a burst. The initial pulse in this case allows the eruptive cloud to overcome the tropopause height. Thus, the formation of a volume of the

positively charged aerosols is impossible due to the positive temperature gradient. As a result of the removal of negatively charged ash particles, a negative volumetric charge is formed in the upper edge of the eruptive cloud, unlike meteorological clouds, in which it is impossible to form a negatively charged upper edge of the cloud without positive cloud–earth lightning, exposing the negative charge on the upper edge of the meteorological cloud [18]. An eruptive cloud with a negatively charged upper edge can rise to the height of the tropopause, and a breakdown into the ionosphere can occur without a breakdown into the ground. At the same time, an uncompensated positive electric charge remains on the lower edge of the eruptive cloud, which then gradually flows down to the earth with the precipitation of positively charged ash.

1.3. The Problems

In the presented work, we were interested in high-altitude discharges, their connection with whistlers, and mechanisms of atmospheric electrification. The waveform of the signal of the VLF radio direction finder allows us to determine the height of the lightning discharge. Thus, WWLLN, AWDANet, and the VLF radio direction finder in the complex, provide the most complete picture of the radio emissions of volcanic thunderstorm activity.

The generation of whistlers by volcanic thunderstorms was shown in [19,20]. In our observations, whistlers are recorded not at a magnetically conjugated point as in [19,20], but after their return from a magnetically conjugated point near volcanoes, the dynamics of the eruption of which is monitored using complex geophysical observations of the KB FRC UGS RAS [21].

Many works have been devoted to the study of volcanic atmospheric-electrical effects [9,11,15,17,22–25]; however, their relationship with the dynamics of eruptive clouds has not been sufficiently studied yet. Observations of whistlers and high-altitude thunderstorms provide additional important information about the features of volcanic eruptions and the formation of eruptive clouds.

With the discovery of high-altitude lightning with their optical images in the form of sprites, jets, and elves, there is a problem of their regular observations not by optical, but by radiophysical methods, which are not limited by weather conditions and time of a day. With the development of radiophysics and electronics, it became possible to observe high-altitude lightning discharges in the VLF radio range with the determination of the spatial distribution of electric currents by methods of solving inverse wave problems.

High-altitude stratospheric electrical discharges, along with tropospheric lightning, play an important role as a regulator in generating the electric potential of the ionosphere and create electromagnetic vibrations in the atmosphere, which coincide with acoustic vibrations in the frequency range, which contributes to the emergence of very complex wave processes in the atmosphere.

The high-altitude electrical discharges and sprites over volcanoes are not unexpected, but there have not yet been reports of observations in the radio range of high-altitude lightning over volcanoes. The presented work is devoted to the development of radiophysical methods for studying high-altitude electrical discharges of meteorological and volcanic origin.

2. Materials and Methods

Recently, the results of studies on the correlation of whistlers and volcanic thunderstorm have been published [19,20]. An analysis of several eruptions of the Okmok and Redoubt volcanoes (Alaska) was presented. During the eruption of the Okmok volcano on 12 July 2008, 21,021 whistlers were recorded at the magnetically conjugated point at the AWDANet Dunedin station. Whistler activity was several times higher than the statistical average daily value, and this suggested that the source of these whistlers is volcanic lightning. This was further confirmed by the correlation between volcanic lightning and whistlers during the eruption of Redoubt volcano in March 2009 [19]. An increase in the number of whistlers was recorded, accompanied by thunderstorm activity within a radius

of 20 km from the volcano, with a total number 808 of whistlers between the first and last explosion. It should be noted that the Okmok and Redoubt volcanoes had different whistler activity. To check this result and to find out the reasons for this difference, it is possible using the eruptions of the Bezymianny and Shiveluch volcanoes in Kamchatka (Russia) in April 2023.

2.1. The Eruptions and Thunderstorm Activity of the Bezymianny and Shiveluch Volcanoes

According to the data of the integrated monitoring of volcanoes of the KB FRC UGS RAS [21] on the Bezymianny volcano on 7 April 2023 at 00:43, 04:00, and 04:45 UTC, there were a series of surface events lasting 3–6 min. At 05:34 UTC, a paroxysmal explosive eruption lasting 16 min began with a maximum eruptive cloud height of up to 9.2 km above sea level (up to 10 km according to satellite data from HIMAWARI-9). Half an hour later, from 06:00 to 24:00, a series of surface events followed, accompanied by ash–gas emissions to an altitude of 5 km above sea level. The VLF complex recorded an increase in electromagnetic radiation in the direction of the Bezymianny volcano (Figure 2a–c).

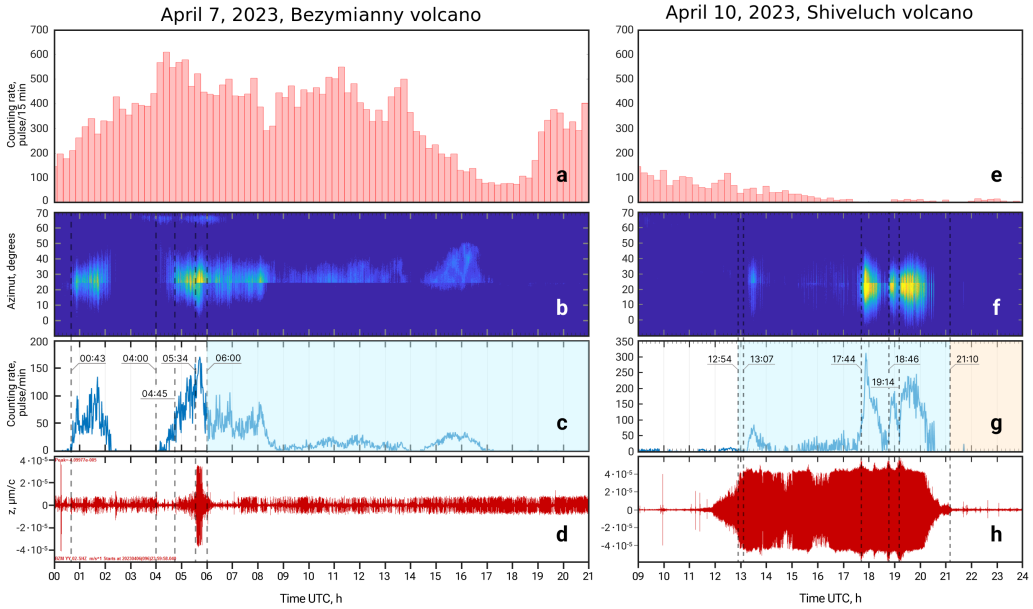

Figure 2. (**a**,**e**) The number of lightning discharges over 15-min time intervals in the area of Australia. (**b**,**f**) Azimuthal distribution of bearings of pulsed electromagnetic radiation in the range of 350°–70°. The count rate of pulsed electromagnetic radiation during eruptions, coming azimuthally from the side of the Bezymianny (**c**) and Shiveluch (**g**) volcanoes. Record of explosive earthquakes at the BZM seismic station during the eruption of the Bezymianny volcano on 7 April 2023 (**d**) and at the BDR seismic station during the eruption of the Shiveluch volcano on 10 April 2023 (**h**).

On 10 April 2023, the Shiveluch volcano became active. At 13:07 UTC on 10 April, an explosive eruption of the Shiveluch volcano began, greatly destroying the lava dome in its crater. According to the Himawari-9 satellite, at 20:30 UTC, the eruptive cloud rose to approximately 20 km. The explosive eruption continued continuously for 3 days, from 10 April to 13 April. The dynamics of the development of ash and aerosol clouds of this eruption are presented in the animations based on the Himawari-8 satellite data from 08:00 UTC on 10 April to 07:50 UTC on 14 April [26]. A detailed description of the eruption is given in [27].

According to remote observations by WWLLN [1], at 13:06 UTC on 10 April 2023, the first warning about the beginning of an explosive eruption of the Shiveluch volcano was received.

According to the VLF direction finder, the onset of thunderstorm activity coincides with the Himawari-9 satellite data. The sharp increase in lightning activity on 10 April

2023 corresponds to the explosions at 17:44, 18:46, and 19:14, recorded by the BDR seismic station. The total number of discharges during the Shiveluch volcano eruption reached 26,101 discharges according to the VLF radio direction finder (Figure 2d–f), while WWLLN recorded only 132 discharges. This difference is due to the peculiarity of the recording of lightning discharges by the WWLLN network [28].

The majority of radio pulses accompanying a volcanic thunderstorm consist of single, short-duration VLF spherics ~97%, and only 3% of VLF spherics are classical lightning with a leader and an extremely low-frequency spheric. WWLLN can detect only these 3% of classical lightning, while the single-point direction finding method used in this study to recognize thunderstorms of the eruptive cloud tracks all radio pulses, which allows determining its size and tracking its movement.

According to WWLLN data, thunderstorm activity was observed in the magnetically conjugated region of Australia during the 7 April 2023 and 10 April 2023 eruptions, as shown in Figures 2 and 3.

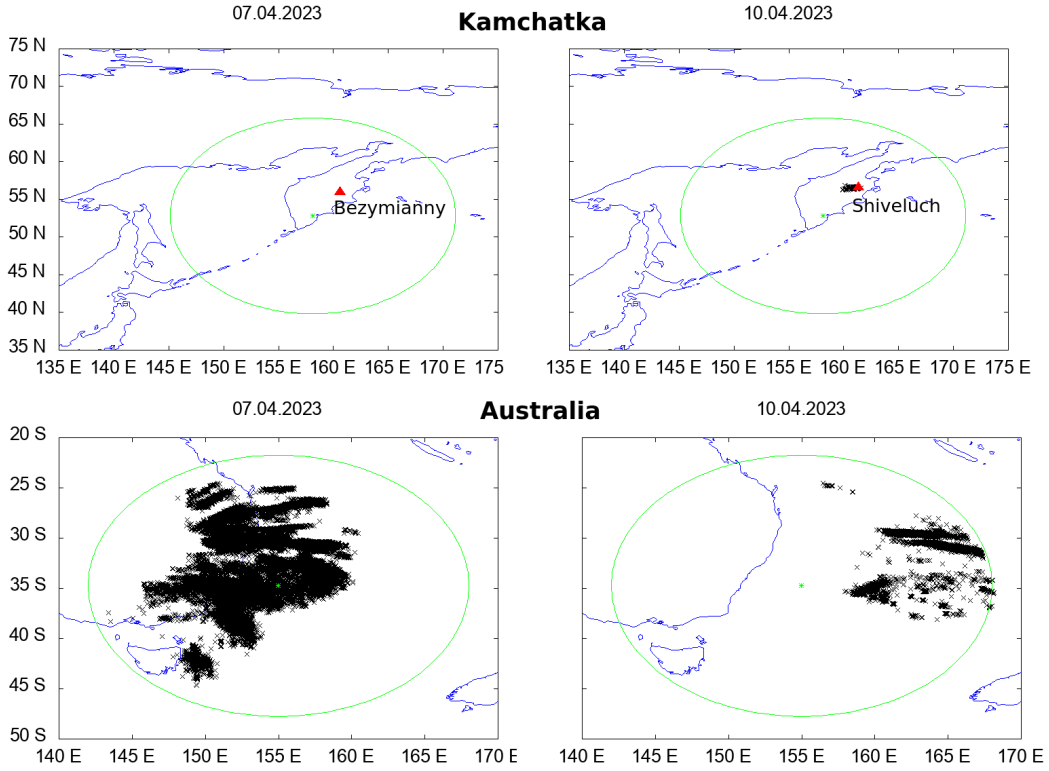

Figure 3. Total daily thunderstorm activity during the eruption of Bezymianny and Shiveluch volcanoes and around their magnetically conjugated regions, x-marker of the lightning stroke.

The maximum of the thunderstorm activity on 7 April 2023 off the coast of Australia coincided with the period of volcanic activity during the eruption of the Bezymianny volcano. Therefore, the VLF direction finder in Kamchatka recorded both one-hop whistlers from Australia and two-hop whistlers generated in Kamchatka. The recorded whistlers from lightning discharges of the Australian thunderstorm center on 7 April 2023 during the eruption of the Bezymianny volcano are shown in coordinates (t, f) in Figure 4a and in coordinates $(t, f^{-1/2})$ in Figure 4b.

2.2. Whistler Recognition

The whistler generation model proposed by [29] suggests that the whistler detected on the ground is caused by a lightning discharge at a magnetically conjugated point, and that multiple reflections at the magnetospheric waveguide boundaries produce an echo with slope coefficients of the straight line $K_i = K/i$, in which $K = D^{-1/2}$, where i is the number of passes along the magnetospheric channel and D is the dispersion coefficient.

According to Storey, whistles with double dispersion coefficient are two-hop whistles. Thus, long whistles with a smaller coefficient K_2 are generated in Kamchatka and reflected over Australia. They travel twice the distance along the magnetospheric channel from Kamchatka to Australia and back. When a powerful lightning discharge occurs near a recording station in Kamchatka during a volcanic eruption, an echo from Australia should be observed with a slope coefficient of the straight line K_2 equal to half the coefficient K_1 of the whistler initiated in the magnetically conjugated region of Australia (diagrams in the insets of Figures 4 and 5) and recorded by the VLF radio direction finder of the IKIR FEB RAS.

For all events of the Bezymianny volcano eruption on 7 April 2023, whistlers with slope coefficients of straight lines $K_1 = (12.5 \pm 1.5) \times 10^{-3} \mathrm{s}^{-1/2}$ and $K_2 = (6.2 \pm 1.5) \times 10^{-3} \mathrm{s}^{-1/2}$ were detected in the VLF direction finder data. Whistlers with coefficients K_1 in Figure 4 are nothing more than whistlers from a thunderstorm center in Australia. This fact is indicated by the absence of an initiating discharge in the VLF direction finder data. On the contrary, a whistler with slope coefficients of straight line $K_2 = (6.2 \pm 1.5) \times 10^{-3} \mathrm{s}^{-1/2}$ has an initiating discharge, from which it can be concluded that this whistler was generated in Kamchatka by a high-altitude discharge of an eruptive cloud.

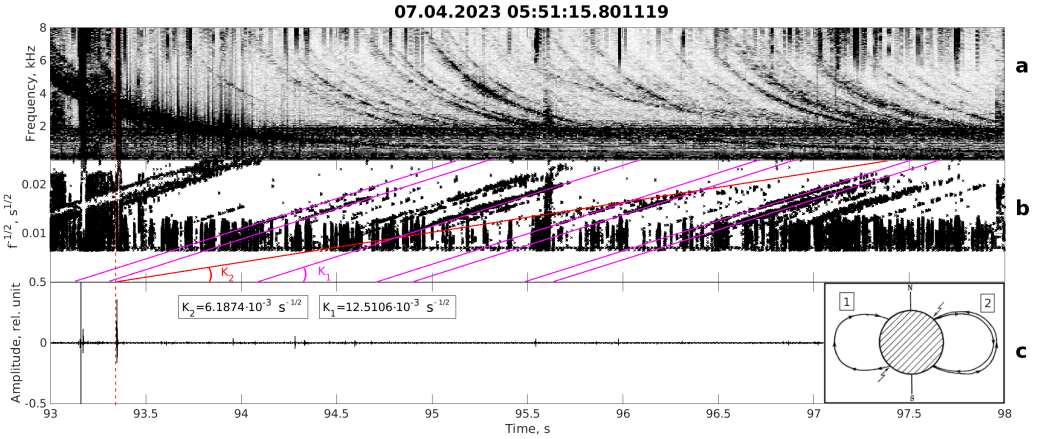

Figure 4. Peak frequencies of the vertical electric component signal of the VLF direction finder during the eruption of Bezymianny volcano on 7 April 2023: (**a**) whistlers initiated by lightning discharges from the Australian thunderstorm center and the eruptive cloud in coordinates (t, f) and (**b**) in coordinates $(t, f^{-1/2})$; (**c**) atmospherics of the initiating thunderstorm discharge of volcanic origin. Slope coefficients $K_1 = (12.5 \pm 1.5) \times 10^{-3} \mathrm{s}^{-1/2}$ and $K_2 = (6.2 \pm 1.5) \times 10^{-3} \mathrm{s}^{-1/2}$. The inset shows the model of electromagnetic wave propagation along a waveguide according to [29]. Time in seconds from the start of the recording is indicated in the figure.

A similar pattern was observed for the eruption of the Shiveluch volcano on 10 April 2023. Figure 5b shows a whistler with $K_2 = (7.6 \pm 1.5) \times 10^{-3} \mathrm{s}^{-1/2}$, indicating the initiating atmospheric (Figure 5c). A distinctive feature of this eruption is that no paired discharges are observed, similar to those recorded on 7 April 2023.

The analysis of data from the eruptions of the Bezymianny and Shiveluch volcanoes over a long period showed that the mechanisms of eruptions of these volcanoes are different; a preliminary description is given in [17]. In our case, we observe the dynamics of two different scenarios for the development of volcanic thunderstorms associated with the formation of an eruptive column and the evolution of an eruptive cloud according to the "soft" scenario for the Bezymianny volcano, in which the eruptive cloud does not reach tropopause heights, and the "hard" scenario with the release of charged negative particles into the stratosphere during the eruption of the Shiveluch volcano.

On 7 April 2023, during the eruption of the Bezymianny volcano, charged ash particles rose to a height of 10 km, while a positive aerosol was formed on the upper edge of the eruptive cloud [9], which prevented the occurrence of high-altitude discharges. In this

case, we observe multiple paired discharges, the first of which is the cloud–earth discharge, and the second is the ionosphere–cloud. The negative charge on the upper edge of the eruptive cloud during the eruption of the Shiveluch volcano on 10 April 2023 is formed directly by an explosion with the removal of negative particles to a height of 20 km, which immediately leads to the formation of a high-altitude discharge.

It is also worth noting that the vertical electrical component of the VLF direction finder for all initiating discharges without exception had a positive initial phase of the first half-wave (Figures 4c and 5c).

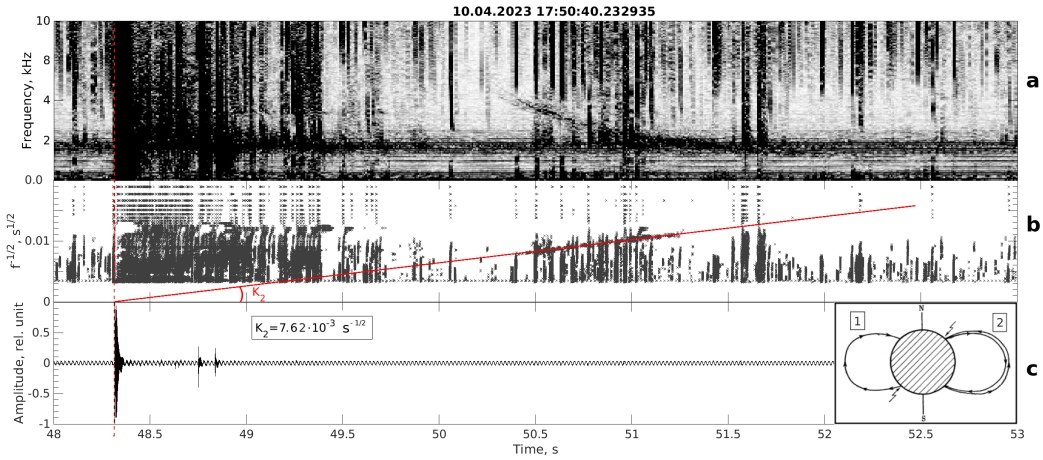

Figure 5. Peak frequencies of the signal of the vertical electrical component of the VLF direction finder during the eruption of the Shiveluch volcano on 10 April 2023: (**a**) whistler initiated by a thunderstorm discharge of an eruptive cloud in coordinates (t, f) and (**b**) in coordinates $(t, f^{-1/2})$; (**c**) atmospherics of the initiating thunderstorm discharge of volcanic origin. The slope coefficient $K_2 = (7.62 \pm 1.5) \times 10^{-3}\text{s}^{-1/2}$.

During the active phase of the Shiveluch volcano explosion, 43 whistling atmospherics were recorded, 25 of which have a straight line slope coefficient $K_2 = (7.6 \pm 1.4) \times 10^{-3}\text{s}^{-1/2}$ (Figure 5b). These whistlers were excited by lightning over Kamchatka. For the remaining eighteen, $K_1 = (16 \pm 2.7) \times 10^{-3}\text{s}^{-1/2}$. These were excited by lightning over Australia.

It is noteworthy that all long whistlers (with a slope coefficient of the straight line $K_2 = (7.6 \pm 1.4) \times 10^{-3}\text{s}^{-1/2}$) coincided with single positive lightning discharges. There were no paired discharges during the eruption of the Shiveluch volcano.

2.3. Determining the Height of the Discharge

To determine the height of the discharge initiating the whistler, an electromagnetic pulse of this discharge (atmospheric) was taken. This pulse was recorded during the eruption of the Shiveluch volcano on 10 April 2023. In accordance with the interferometry scheme shown in Figure 6a, a technique was used to determine the height h of the discharge by the delay time τ between atmospheric pulses, direct and reflected from the ionosphere. The geometry of the ray path difference is shown in Figure 6b. The difference ΔL in the path of the rays is a function of the height of the waveguide H, the horizontal projection of the distance to the discharge L, and the height of the discharge h . The parameters H and L can be determined from experimental data: H is found from the cutoff frequency of the waveguide and L is the distance to the volcano.

The spectral function (Figure 6b) of the atmospheric H recorded on 10 April 2023 at 17:51:28.5489 UTC is used for the determination of H. The cutoff frequency in this case is 1.7 kHz. The corresponding half-wave length, equal to the height of the waveguide, is 88 km. Thus, we get $H = 88$ km. The projection of the distance to the discharge L is assumed to be equal to the distance to the Shiveluch volcano ± 50 km. The uncertainty of ± 50 km arises due to the size of the eruptive cloud taken from Himawari-9 satellite data.

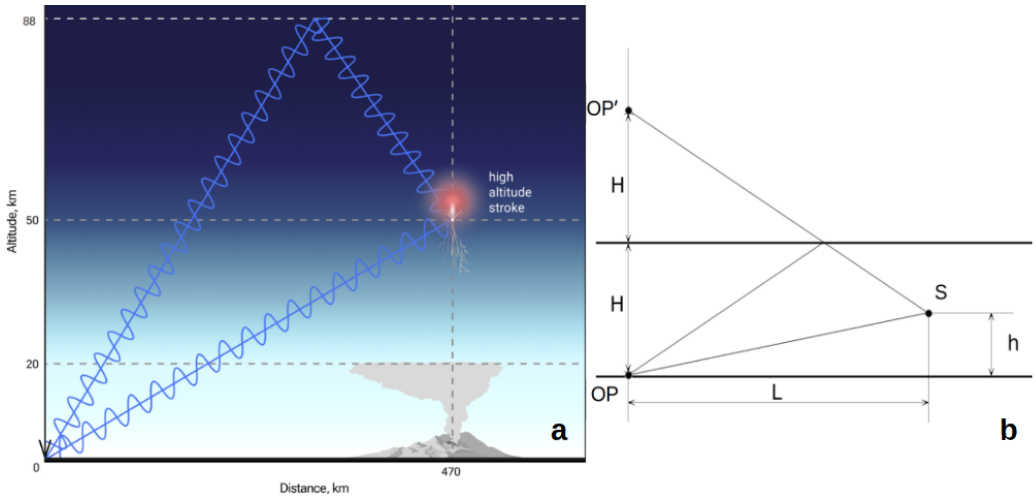

Figure 6. (**a**) An interferometry scheme for determining the height of the discharge. (**b**) The geometry of the difference in the paths of the atmospheric rays during the eruption of the Shiveluch volcano. The symbols 0 and OP indicate the observation point "Karymshina".

According to Figure 6b, the path difference of the rays is $\Delta L = \sqrt{L^2 + (2H - h)^2} - \sqrt{L^2 + h^2}$, and the delay time is $\tau(h) = \Delta L(h)/c$. Under conditions $0 < h < H$ and $h, H \ll L$, in the first approximation $\Delta L(h) \simeq 2H(H - h)/L$.

The signal amplitude at the reception point is $A_{OP} = A_S + A_R \cdot e^{i\omega\tau}$, where A_S and $A_R \cdot e^{i\omega\tau}$ are the amplitudes of the source and its reflection from the ionosphere, $\omega = 2\pi f$, where f is the frequency of the source. Considering that the path difference is not large, $A_S \simeq A_R$, and therefore, $A_{OP} = A_S + A_R \cdot e^{i\omega\tau} \simeq A_S(1 + e^{i\omega\tau})$, and for the signal intensity at the reception point, depending on the height of the source h, we obtain $|A_{OP}|^2 \simeq 2|A_R|^2(1 + \cos(\omega\tau(h)))$.

This model power spectrum, shown in Figure 7a, can be compared with the real signal power spectrum at the receiver point (Figure 7b). Their correlation function (convolution) is shown in Figure 7c. The maximum correlation at $h = 52$ km determines the height of the source. We obtained the height of the stratopause, where the temperature has a local maximum which apparently contributes to the electrical discharge.

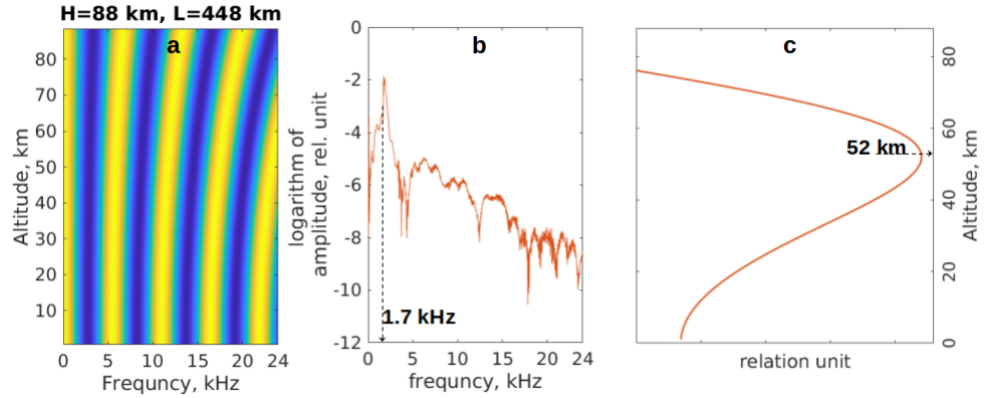

Figure 7. (**a**) Interferogram of the model power spectrum for determining the discharge height, (**b**) Power spectrum of the real atmospheric signal recorded at the reception point at 17:51:28.5489 UTC during the eruption of the Shiveluch volcano on 10 April 2023. (**c**) Correlation function (convolution) of the model and real signal spectra.

Based on the results of data processing for 25 discharges that excited whistlers with a coefficient of $K_2 = (7.6 \pm 1.4) \times 10^{-3} \mathrm{s}^{-1/2}$; the height of the lightning discharge was

confirmed to be more than 40 km, and the correlation of the signal spectra in Figure 7c can be considered as the altitude distribution of the discharge.

The pattern for the high-altitude discharge during the eruption of the Bezymianny volcano will be the same, since the atmospheric of the high-altitude discharge in both cases has the same shape, which is determined by the properties of the atmosphere at the height of the stratopause, where the temperature has a local maximum.

3. Results

The analysis of the eruptions of the Bezymianny and Shiveluch volcanoes in Kamchatka (Russia) in April 2023 revealed a connection between lightning and whistlers recorded by the VLF radio direction finder at the Karymshina station.

The results of the analysis of the characteristics of high-altitude electrical discharges were associated with the type of eruption of the Bezymianny and Shiveluch volcanoes.

Based on the observations of atmospherics and whistlers excited by high-altitude electrical discharges that occurred during the eruptions of the Bezymianny and Shiveluch volcanoes in Kamchatka (Russia) on 7 and 10 April 2023, data were obtained on the height of electrical discharges and the region of whistler generation.

Two-hop whistlers generated in Kamchatka were determined by the dispersion coefficient, which corresponded to a double pass of the signal from Kamchatka to Australia and back.

The heights of electrical discharges were determined using interferograms of direct and reflected from the ionosphere radio rays of the atmospheric.

The altitude distribution (Figure 7c) of the electrical discharge, the penetration of which into the ionosphere is responsible for the generation of whistlers, was obtained.

Characteristics of volcanic electrical discharges and whistlers can be used to estimate the height of an explosive eruption. The paired high-altitude electrical discharge is associated with a "soft" scenario of the volcanic eruption. The single high-altitude electrical discharge is associated with a "hard" scenario of the volcanic eruption.

4. Discussion

Since there is no observation in the optical range, high-altitude electrical discharges accompanying volcanic eruptions were recorded only by a VLF direction finder, and their height was confirmed by the developed method.

Electrification of the atmosphere remains an urgent problem in the studies of thunderstorm activity related to height lightning discharges, in spite of the fact that many papers have been published which describe the mechanisms of sprites formation and generation [30]. The classical mechanisms of formation of high-altitude electrical discharges in meteorological thunderstorms described in [31] are also possible in volcanic thunderstorms with a "soft" eruption scenario (most eruptions of Bezymianny volcano) [32]. Another mechanism occurs during eruptions of the Shiveluch volcano, which has not been described yet. It is assumed that in the case of a "hard" eruption scenario, the uncompensated negative electrical charge is transferred above the tropopause due to the explosion process and causes an electrical breakdown in the ionosphere, i.e., a high-altitude electrical discharge between the ionosphere and the eruptive cloud.

5. Conclusions

Due to the explosive process of volcanic eruption, eruptive clouds, unlike meteorological ones, can overcome the tropopause. As a result, charged ash is carried to a significant height, creating all the conditions for the occurrence of a high-altitude electrical discharge, which simultaneously initiates an atmospheric, a whistler, and a sprite. The height of the discharge coincides with the stratopause region with a local maximum temperature. The role of this area requires closer attention in the future. In addition, the mechanism of penetration of a high-altitude electric discharge into the ionosphere, which creates plasma oscillations in the magnetosphere, requires more detailed research.

Author Contributions: Conceptualization, E.I.M.; methodology, B.M.S. and J.L.; software, E.I.M. and E.A.K.; validation, E.I.M. and E.A.K.; formal analysis, E.I.M.; investigation, E.I.M. and N.V.C.; data curation, E.I.M. and J.L.; writing—original draft preparation, E.I.M., N.V.C., and B.M.S.; writing—review and editing, J.L. and B.M.S.; visualization, E.I.M., E.A.K., and N.V.C.; supervision, B.M.S. All authors have read and agreed to the published version of the manuscript.

Funding: The work was supported by the IKIR FEB RAS State Task (subject registration No. 124012300245-2) and by the TKP2021-NVA-29 project, with support provided by the Ministry of Culture and Innovation of Hungary from the National Research, Development and Innovation Fund.

Institutional Review Board Statement: Not applicable.

Informed Consent Statement: Not applicable.

Data Availability Statement: The raw data supporting the conclusions of this article will be made available by the authors on request.

Conflicts of Interest: The authors declare no conflicts of interest.

References

1. World Wide Lightning Location Network. Available online: http://wwlln.com (accessed on 13 December 2024).
2. IKIR FEB RAS Cite. Available online: https://www.ikir.ru (accessed on 13 December 2024).
3. James, M.; Wilson, L.; Lane, S.; Gilbert, J.; Mather, T.; Harrison, R.; Martin, R. Electrical charging of volcanic plumes. *Space Sci. Rev.* **2008**, *137*, 399–418. [CrossRef]
4. Ewert, J.W.; Holzworth, R.H.; Diefenbach, A.K. Global detection of explosive volcanic eruptions with the World Wide Lightning Location Network (WWLLN) and application to aviation safety (Invited). In *AGU Fall Meeting Abstracts*; Art. No. AE31A-04; U.S. Geological Survey: Vancouver, WA, USA, 2010; Volume 2010.
5. Van Eaton, A.R.; Amigo, Á; Bertin, D.; Mastin, L.G.; Giacosa, R.E.; González, J.; Valderrama, O.; Fontijn, K.; Behnke, S.A. Electrical charging of volcanic plumes. *Geophys. Res. Lett.* **2016**, *43*, 3563–3571. [CrossRef]
6. Briggs, M.S.; Lesage, S.; Schultz, C.; Mailyan, B.; Holzworth, R.H. A terrestrial gamma ray flashfrom the 2022 Hunga Tonga volcanic eruption. *Geophys. Res. Lett.* **2022**, *49*, e2022GL099660.
7. Lichtenberger, J.; Ferencz, C.; Bodnar, L.; Hamar, D.; Steinbach, P. Automatic Whistler Detector and Analyzer system: Automatic Whistler Detector. *J. Geophys. Res.* **2008**, *113*, A12201. [CrossRef]
8. AWDANet, PLASMON. Available online: http://plasmon.elte.hu/awdanet.htm (accessed on 13 December 2024).
9. Rulenko, O.P.; Tokorev, P.I. Atmospheric-electric effects of the Large fractured Tolbachinsky eruption in July–October 1975. *Bull. Volcanol. Stn.* **1979**, *56*, 96–102.
10. Miura, T.; Koyaguchi, T.; Tanaka, Y. Measurements of electric charge distribu-tion in volcanic plumes at Sakurajima Volcano. *Jpn. Bull. Volcanol.* **2002**, *64*, 75–93.
11. Mather, T.A.; Harrison, R.G. Electrification of volcanic plumes. *Surv. Geophys.* **2006**, *27*, 387–432. [CrossRef]
12. Méndez, Harper, J.; Cimarelli, C.; Cigala, V.; Kueppers, U.; Dufek, J. Charge injection into the atmosphere by explosive volcanic eruptions through triboelectrification and fragmentation charging. *Earth Planet. Sci. Lett.* **2021**, *574*, 117162. [CrossRef]
13. Behnke, S.A.; Edens, H.E.; Thomas, R.J.; Smith, C.M.; McNutt, S.R.; Van Eaton, A.R.; Cimarelli, C.; Cigala, V. Investigating the origin of continual radio frequency impulses during explosive volcanic eruptions. *J. Geophys. Res. Atmos.* **2018**, *123*, 4157–4174. [CrossRef]
14. Van Eaton, A.R.; Schneider, D.J.; Smith, C.M.; Haney, M.M.; Lyons, J.J.; Said, R.; Fee, D.; Holzworth, R.H.; Mastin, L.G. Did ice-charging generate volcanic lightning during the 2016–2017 eruption of Bogoslof volcano, Alaska? *Bull. Volcanol.* **2020**, *82*, 24. [CrossRef]
15. Arason, P.; Bennett, A.J.; Burgin, L.E. Charge mechanism of volcanic lightning revealed during the 2010 eruption of Eyjafjallajökull. *J. Geophys. Res.* **2011**, *116*, 387–432. [CrossRef]
16. Lane, S.; Gilbert, J.; Kemp, A.J. Electrical and chemical properties of eruption plumes at Sakurajima volcano, Japan. In *8th Report of Geophysical and Geochemical Observations at Sakurajima Volcano, Sakurajima Volcanological Observatory*; Kyoto University: Kyoto, Japan, 1995; pp. 105–127.
17. Malkin, E.; Cherneva, V.; Makhlai, D.; Cherneva, N.; Sannikov, D.; Druzhin, G.; Akbashev, R.; Holzworth, R. Analysis of Electromagnetic Radiation During Shiveluch and Bezymyanniy Volcano Eruptions from 2017 to 2023. In Proceedings of the International Conference Solar-Terrestrial Relations and Physics of Earthquake Precursors, Kamchatka, Russia, 25–29 September 2023; Springer Nature Switzerland: Cham, Switzerland, 2023; pp. 62–70.
18. Winckler, J.R. The cloud–ionosphere discharge: A newly observed thunderstorm phenomenon. *Proc. Natl. Acad. Sci. USA* **1997**, *94*, 10512–10519. [CrossRef] [PubMed]
19. Collier, A.B.; Bremner, S.; Lichtenberger, J.; Downs, J.R.; Rodger, C.J.; Steinbach, P.; McDowell, G. Global lightning distribution and whistlers observed at Dunedin, New Zealand. *Ann. Geophys.* **2010**, *28*, 499–513. [CrossRef]

20. Antel, C.; Collier, A.B.; Lichtenberger, J.; Rodger, C.J. Investigating Dunedin whistlers using volcanic lightning. *Geophys. Res. Lett.* **2014**, *41*, 4420–4426. [CrossRef]
21. Geophysical Survey RAS Monitoring Data. Available online: http://www.emsd.ru/~ssl/monitoring/main.htm (accessed on 13 December 2024).
22. Holzworth, R.H.; Winglee, R.M.; Barnum, B.H.; Li, Y.; Kelley, M.C. Lightning whistler waves in the high-latitude magnetosphere. *J. Geophys. Res.* **1999**, *104*, 17369–17378. [CrossRef]
23. Thomas, R.J.; Krehbiel, P.R.; Rison, W.; Edens, H.E.; Aulich, G.D.; Winn, W.P.; McNutt, S.R.; Tytgat, G.; Clark, E. Electrical activity during the 2006 Mount St. Augustine volcanic eruptions. *Science* **2007**, *315*, 1097. [CrossRef]
24. McNutt, S.; Williams, E. Volcanic lightning: Global observations and constraints on source mechanisms. *Bull. Volcanol.* **2010**, *72*, 1153–1167. [CrossRef]
25. Behnke, S.A.; Thomas, R.J.; McNutt, S.R.; Schneider, D.J.; Krehbiel, P.R.; Rison, W.; Edens, H.E. Observations of volcanic lightning during the 2009 eruption of Redoubt volcano. *J. Volcanol. Geotherm. Res.* **2013**, *259*, 214–234. [CrossRef]
26. Dynamics of Development of Ash and Aerosol Clouds. Available online: http://d33.infospace.ru/jr_d33/materials/2023v20n2/283-291/1683110898.webm (accessed on 13 December 2024).
27. Girina, et.al. Analysis of the development of the paroxysmal eruption of Sheveluch volcano on April 10–13, 2023, based on data from various satellite systems. *Sovrem. Probl. Distantsionnogo Zondirovaniya Zemli Kosmosa* **2023**, *20*, 283–291. [CrossRef]
28. Dowden, R.L.; Brundell, J.B.; Rodger, C.J. VLF lightning location by time of group arrival (TOGA) at multiple sites Source. *J. Atmos.-Sol.-Terr. Phys.* **2002**, *64*, 817–830. [CrossRef]
29. Storey, L.R.O. An investigation of whistling atmospherics. *Philos. Trans. R. Soc. Lond.* **1953**, *246*, 113–141.
30. Pasko, V.P.; Inan, U.S.; Bell, T.F.; Taranenko, Y.N. Sprites produced by quasi-electrostatic heating and ionization in the lower ionosphere. *J. Geophys. Res.* **1997**, *102*, 4529–4561. [CrossRef]
31. Pasko, V.P.; Yair, Y.; Kuo, C.L. Lightning Related Transient Luminous Events at High Altitude in the Earth's Atmosphere: Phenomenology, Mechanisms and Effects. *Space Sci. Rev.* **2012**, *168*, 475–516. [CrossRef]
32. Malkin, E.I.; Cherneva, V.I.; Makhlai, D.O.; Cherneva, N.V.; Akbashev, R.R.; Sannikov, D.V. Remote methods for observations of Shiveluch and Bezymianny volcano eruptions. *Vestnik Kraunc. Fiz.-Mat. Nauki.* **2023**, *43*, 141–165.